Automatic Grasp Generation for Vacuum Grippers for Random Bin Picking

Muhammad Usman Khalid[1], Felix Spenrath[1], Manuel Mönnig[1], Marius Moosmann[1], Richard Bormann[1], Holger Kunz[2], and Marco F. Huber[1,3]

[1] Fraunhofer Institute for Manufacturing Engineering and Automation IPA, Stuttgart, Germany,
muk@ipa.fhg.de, fps@ipa.fhg.de
[2] FORMHAND Automation GmbH
[3] Institute of Industrial Manufacturing and Management IFF, University of Stuttgart, Germany.

Abstract. In random bin picking, grasps on a workpiece are often defined manually, which requires extensive time and expert knowledge. In this paper, we propose a method that generates and prioritizes grasps for vacuum and magnetic grippers by analyzing the CAD model of a workpiece and gripper geometry. Using projections of these models, heatmaps such as the overlap of gripper and workpiece, the center of gravity, and the surface smoothness are generated. To get a combined heatmap, which estimates the probability for a successful grip, all individual heatmaps are fused by means of a weighted sum. Grid-based sampling generates prioritized grasps and suggests the most suitable gripper automatically. This approach increases the autonomy of bin picking significantly.

Keywords: bin picking, computer vision, grasp generation

1 Introduction

In manufacturing industry, workpieces are often stored chaotically in bins. However, for many processing steps, the workpieces have to be separated, e.g., to be fed to a production machine. This is still mostly done manually, especially for large workpieces, but robots are nowadays used extensively for this task, which is called *bin picking* [10]. Bin picking is a highly researched topic and there are two different approaches: model-free and model-based. Model-free approaches search for possible grasps in the sensor data of the filled bin without using a model of the workpiece [6]. Since the pose of the workpiece is not known, these approaches struggle with a precise placement of the workpieces. In contrast, model-based approaches use a model of the workpiece to determine the pose of each workpiece inside the bin [9]. After the pose has been determined, a collision free robot path has to be calculated to extract each workpiece, e.g., by using a heuristic search algorithm [1][2]. To calculate the appropriate robot movement, the system has to know how the workpiece can be grasped. Since the orientation of the part is arbitrary in bin picking scenarios, many different grasp candidates are required.

For working with new variants of workpieces, the definition of such grasps (target point on workpiece and approaching vector) can still be defined manually. However, it requires expert knowledge and manual labor for each workpiece, which is unpractical for a large variety of different workpieces. This paper proposes an approach to automatically generate these grasps for suction grippers, focusing on form-flexible suction grippers like FormHand [8]. While the goal of this paper is to generate grasps for bin picking, the technology can also be used for any other handling tasks, e.g., conveyor picking.

After a review of the state of the art in Section 2, the calculation of a heatmap that represents the probability of grasping success is developed in Section 3. In Section 4, we describe a method to generate discrete grasps based on this heatmap. Finally, the results are compared with physical experiments in Section 5. The main contributions of this paper are as follows:

- Generation of a heatmap that represents the probability of grasping success based on projections of the workpiece. This heatmap considers several factors like overlapping between the workpiece and the gripper, the surface smoothness, and the center of gravity.
- Generation of discrete grasps on the workpiece and the selection of the most suitable gripper for a workpiece.

2 Related Work

While there is a considerable amount of work on generating suitable grasps for clamping grippers [3–5], suction cup grippers are not studied that much. Kraft et al., [7] generate grasps for clamping grippers and suction cup grippers by randomly distributing the grasps on the workpiece and calculating a value for the grasp quality. The generated grasps are validated and prioritized using simulation to learn which grasps are more successful than others. Mahler et al., [6] generate grasps for suction cup grippers by using a quasi-static spring model. However, most of these approaches make the assumption that the grippers can not grip if there is even a small hole in the gripping area, which is quite common, e.g., with sheet metal parts. However, there are more flexible suction grippers, like FormHand, which can grip, even in the presence of holes [8]. This paper therefore focuses on generating grasps for such a robust suction gripper on generally flat parts like sheet metal parts.

3 Probability Matrix of a Successful Grasp

3.1 Projection of Workpiece and Gripper

Instead of calculating all the property matrices of gripper and workpiece directly from a CAD model, we use 2D projection matrices for both gripper and workpiece. For a gripper, we project it only from its top view so that the contact surface of gripper can be projected to an image plane as shown in Figure 1(a,b).

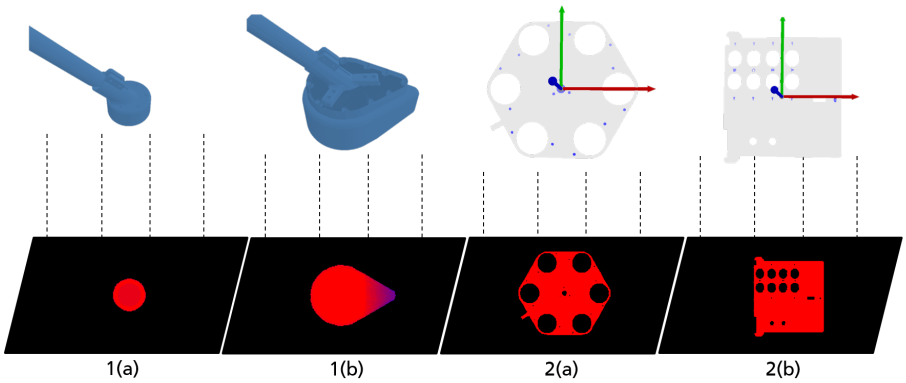

Fig. 1. Gripper and workpiece projections on 2D images. 1(a) Projection of a small gripper. 1(b) Projection of a large gripper. 2(a) Projection of a hexagonal type workpiece. 2(b) Projection of a rectangular workpiece.

This projection P_g works for all types of vacuum grippers consisting of any number of suction cups and also for magnetic grippers. In the similar manner, the CAD model of the workpiece is projected to a 2D image as shown in Figure 1(c,d). This projection values represent the depth value of workpiece in each pixel. As our scope of work consists of flat workpieces, we project the workpiece from all its 6 sides. However, to speed up the process of grasps generation, some projections can be discarded at the start of the process by using the valid pixels V_p in the top projection. By comparing the valid pixels in each projection with V_p and using 60% as threshold, some projections can be discarded at the start of the process. In our test set, threshold was found by physically examining the geometry of workpieces.

3.2 Overlap between Workpiece and Gripper

To find the contact surface area between gripper and workpiece, an overlap heatmap is calculated using projections of gripper and workpiece. The center pixel of gripper projection P_g is taken as an anchor point p_a. With respect to the anchor point, the gripper projection P_g is traversed pixel by pixel over the workpiece projection P_w. For each traversal, the number of pixels of workpiece for which gripper pixels have non-zero value are calculated. This defines the heatmap H_o of overlap between gripper and workpiece, as shown in Figure 2(b). To calculate the overlapping, the gripper and workpiece projections are binarized:

$$b_w(x,y) = \begin{cases} 1 & \text{if } P_w(x,y) \neq 0 \\ 0 & \text{otherwise} \end{cases}, \; b_g(x,y) = \begin{cases} 1 & \text{if } P_g(x,y) \neq 0 \\ 0 & \text{otherwise} \end{cases} \tag{1}$$

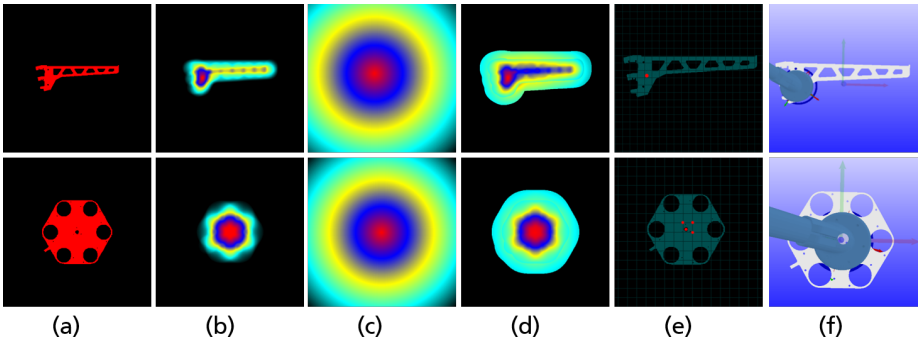

Fig. 2. Calculation of grasp reliability matrix and generation of gripping points for W5 and W6. (a) Projection of workpiece. (b) Overlapping heatmap of workpiece and gripper pixels. (c) heatmap of centre of gravity. (d) Weighted combination of heatmaps. (e) Grid based discrete grasp pixels. (f) Generated grasps.

For a specific point (x, y) in the workpiece projection P_w, the overlap $H_o(x, y)$ at this point is then calculated as the convolution of b_w with b_g:

$$H_o(x,y) = \sum_{i=1}^{w_g} \sum_{j=1}^{h_g} b_w(x - c_x + i, y - c_y + j) \cdot b_g(i,j) \quad \text{for} \quad c_x < x < w_w - c_x \quad , \quad c_y < y < h_w - c_y \tag{2}$$

with the width w_g, the height h_g, and the center pixel (c_x, c_y) of the gripper projection and the width w_w, the height h_w of workpiece projection. To calculate the effectiveness of overlapping with respect to workpiece and gripper sizes, overlap heatmaps are normalized with respect to gripper H_{og} and workpiece H_{ow} by dividing overlap heatmaps with number of non-zero pixels in the gripper and workpiece projection, respectively.

3.3 Calculation of Center of Gravity Heatmap

It is desirable to pick the workpiece from its centre of gravity because it ensures that the weight of part is evenly divided and with firm gripping, the workpiece is less likely to drop. Therefore, we also introduced a centre of gravity heatmap into the calculation of grasp reliability matrix. For calculating the centre of gravity, we assumed that the part is uniformly thick and made of the same material. The centre of gravity pixel p_{cog} is calculated by adding all the x and y valid values in workpiece projection P_w and dividing it by total number of non-zero pixels. For a pixel at (i, j), heatmap for centre of gravity $H_{cog}(i, j)$ is calculated as

$$H_{cog}(i,j) = \max(H_{cog}) - \sqrt{(x_i - x_{cog})^2 + (y_j - y_{cog})^2} \ , \tag{3}$$

where $\max(H_{cog})$ is the maximum value in centre of gravity heatmap. Figure 2(c) shows the heatmap for centre of gravity.

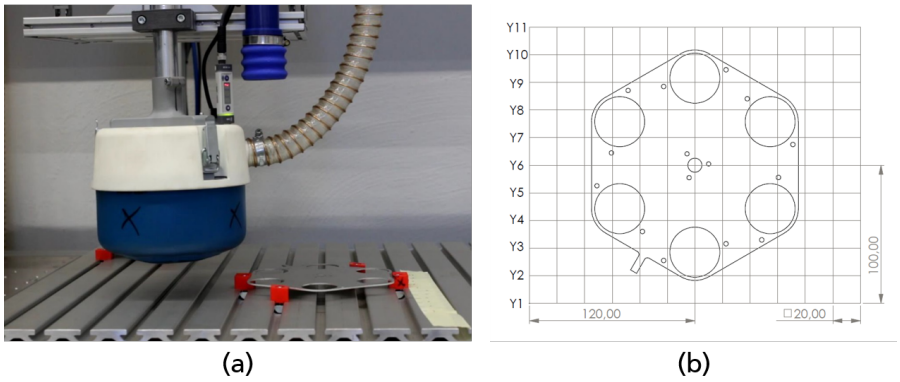

Fig. 3. Measurement of vacuum pressure with gripper. (a) Setup for measuring vacuum pressure. (b) Grid for measuring at different points on workpiece.

3.4 Calculation of Surface Smoothness

Some workpieces have grooves on their surface and when a vacuum gripper grasp the workpiece at that point, leakage of vacuum occurs and the workpiece is dropped during grasping. Therefore, it is important to find a matrix that provides the information of grooves or humps. We calculate a surface smoothness heatmap to consider these properties in our calculation of grasping points. Similar to the calculation of overlap heatmap, the heatmap for surface smoothness H_s is calculated by traversing pixel by pixel over workpiece projection P_w and calculating the sum of differences between z-surface value and z-value in workpiece projection.

3.5 Weighted Combination and Normalization of Matrices

To incorporate the influence of all property matrices of gripping, a weighted combination of heatmaps is calculated. To get the uniform influence of heatmaps in the combined heatmap, each heatmap is normalized with respect to its maximum value. The combined heatmap H_c is calculated as

$$H_c = w_{og} \cdot \tilde{H}_{og} + w_{ow} \cdot \tilde{H}_{ow} + w_{cog} \cdot \tilde{H}_{cog} + w_s \cdot \tilde{H}_s \tag{4}$$

Here, w_{og} tends to change the sensitivity of heatmap w.r.t the gripper. Heatmap H_{og} is defined in a way that a smaller workpiece with smaller gripper has higher heatmap H_{og} values as compared to a smaller workpiece with a larger gripper. Moreover, w_{ow} tends to change the sensitivity of heatmap w.r.t the workpiece. Heatmap H_{ow} is defined in a way that a smaller workpiece with larger gripper have higher heatmap H_{ow} values as compared to a smaller workpiece with smaller gripper. By adjusting the weights w_{og} and w_{ow}, a suitable gripper for a workpiece can be selected.

4 Grasps Generation and Gripper Selection

The heatmap is a continuous representation of grasp regions. However, for the generation of grasps, the heatmap has to be discretized. The heatmaps are discretized in a manner that the grasps are evenly distributed over the image with a certain distance in between. Moreover, we have extended our approach to suggest the best gripper from selection.

4.1 Gripper Selection

For some workpieces, particularly having holes, it is not easy to decide which gripper would be the most suitable one for that workpiece. We extend our approach of grasp probability matrices to suggest the suitable gripper from the selection. The heatmap H_{og} defines how well the gripper surface is overlapped with workpiece one. The greater the value of H_{og}, the greater is the contact surface of gripper on workpiece. On the other hand, heatmap H_{ow} defines how much surface area of workpiece is overlapped by the gripper. The gripper that receives the maximum score for the combination of these heatmaps is selected for a workpiece.

4.2 Generation and Prioritization of Grasps

For the generation of grasps from heatmap H_c, we use grid based discretization. Based on the bounding box of workpiece, a grid is generated with fixed width g_w and height g_h. Within each grid cell, the grasp pixel with maximum score is calculated. However, these grasp pixels can be very close to each other and not uniformly distributed over workpiece surface. Therefore, we applied a two step filtration of grasp pixels. In the first step, the grid pixels are sorted based on their heatmap scores. In the second step, a grid pixel is checked sequentially with its neighboring grid grasp pixels. If the distance between neighbouring grasp pixels is less than half of the grid width, the grid pixel with lower score is discarded. After the filtration of closely neighbored grasp pixels, grasps $p_g(x, y, z, \alpha, \beta, \gamma)$ are generated in which (x, y) are taken from pixel position of the heatmap, z is taken from depth value of grasp pixel in workpiece projection P_w and approach vector (α, β, γ) is taken from normal vector to the grasp pixel plane. Grasps are then converted to a transformation matrix T_p^g of grasp in pixel coordinate system, which is then transformed to its object coordinate system as $T_o^g = T_o^p \cdot T_p^g$. Here T_o^p is the transformation of object in pixel coordinate system as defined during workpiece projection W_p.

5 Experiments and Results

5.1 Hardware Testing Setup

We have arranged an experimental setup in our lab, as shown in Fig. 3. In our hardware setup, we fix the workpiece slightly elevated above from the base table to allow for free airflow through cut-outs in the workpiece simulating the

Table 1. Evaluation of grasp reliability heatmaps and gripper selection on test set

Workpiece	**Gripper**	**Correlation**	**Maximum pressure**	**Maximum overlapping**
W1	Small	0.53	244	312.99
W2	Small	0.76	214	452.83
W3	Small	0.71	211	384.59
W4	Small	0.73	210	202.81
W5	Small	0.73	291	459.24
W6	Small	0.81	**360**	**459.24**
W6	Large	0.75	270	436.56
W7	Small	0.60	421	459.03
W7	Large	0.74	**458**	**459.13**
W8	Small	0.76	379	459.26
W9	Small	0.95	242	440.22
W10	Small	0.71	242	454.83
Average		**0.73**		

situation after picking. The form-flexible suction gripper is positioned on the workpiece in a grid by a linear axis system and the resulting vacuum pressure [mbar] is measured. We chose a grid size of 10-20 mm resulting in up to 70 measurement points depending on the workpiece. The measurement was repeated five times at every position. The points where we get higher vacuum pressure are likely to be better points for the gripper to grasp that object.

5.2 Evaluation of Grasp Reliability and Gripper Selection

To validate our generated grasp reliability heatmaps, we compare the overlap heatmap H_o with the vacuum pressure recorded in physical experiments, described in Section 5.1. We calculated overlap score at each point defined in the grid for each workpiece, shown in Figure 3(b). Pearson correlation coefficient is calculated for all the points of overlap with vacuum pressure and recorded in Table 1. A higher correlation coefficient closer to 1 shows that our algorithm is well correlated with grasp reliability in physical experiments. As the workpiece was fixed in our experiments, centre of gravity did not play any role in the measurements. Therefore, the correlation coefficient was calculated only with overlap heatmap.

Moreover, for the generation of combined heatmap of grasp reliability, we use $w_{og} = 1.8$, $w_{ow} = 0.01$, $w_{cog} = 1.5$, and $w_s = 0.5$. These weights were found empirically by comparing the heatmaps with the measured heatmaps of Section 5.1 of a subset of the test set. The weights w_{og}, w_{ow} are more sensitive for the selection of a suitable gripper and the weights w_{cog}, w_s are more sensitive with respect to the geometry of the workpiece. Also, as most of the workpieces have smooth surfaces, therefore, w_s has very little effect on combined heatmap. By fixing these weights, combined heatmaps for the complete test set are recorded and listed in Table 1. A total of 10 workpieces are tested with a small gripper and

$W6$ and $W7$ also with a larger gripper. In physical experiments, it was observed that the small gripper is suited for $W6$ and a larger one for $W7$. We observe the similar trend in our combined reliability matrix. This result shows that our algorithm can choose the best suitable gripper from the available options. Also, we have applied our generated grasps successfully in the experimental setup of bin picking, details are provided in the supplementary material.

By using the speedup option of valid pixels V_p defined in Section 3.1, the average time for grasp generation is around 5.5 seconds on CPU Core i5-5200 @ 2.20GHz, 8GB. As our algorithm is deterministic and does not depend upon randomness, the same grasps can be generated repeatedly in the setup when weights and grid size are fixed in settings.

6 Conclusion

We presented a novel approach to generate grasps for a form-flexible suction gripper on generally flat workpieces like sheet metal parts. These grasps can be used for bin picking applications, where a lot of different grasps are needed due to the arbitrary placement of each workpiece. The results show that this approach can generate suitable grasps and determine an overlapping score which correlates well with physical experiments. Future work may include extending the approach to 3d objects and applying it to model-free grasping system.

References

1. Spenrath, F., & Pott, A. (2017). Gripping point determination for bin picking using heuristic search. Procedia CIRP, 62, 606-611.
2. Spenrath, F., & Pott, A. (2018, August). Using Neural Networks for Heuristic Grasp Planning in Random Bin Picking. In 2018 IEEE (CASE).
3. Miller, A. T., & Allen, P. K. (2004). Graspit! a versatile simulator for robotic grasping. IEEE Robotics & Automation Magazine, 11(4), 110-122.
4. Jørgensen, J. A., & Petersen, H. G. (2008) . Usage of simulations to plan stable grasping of unknown objects with a 3-fingered Schunk hand. In IEEE/RSJ.
5. Mahler, J., Pokorny, F. T., Hou, B., Roderick, M., Laskey, ... & Goldberg, K. (2016, May). Dex-net 1.0: A cloud-based network of 3d objects for robust grasp planning using a multi-armed bandit model with correlated rewards. In IEEE ICRA.
6. Mahler, J., Matl, M., Liu, X., Li, A., Gealy, D., & Goldberg, K. (2018, May). Dex-Net 3.0: Computing robust vacuum suction grasp targets in point clouds using a new analytic model and deep learning. In IEEE ICRA.
7. Kraft, D., Ellekilde, L. P., & Jørgensen, J. A. (2014). Automatic grasp generation and improvement for industrial bin-picking. In Accelerating Cross-fertilization between Academic and Industrial Robotics Research in Europe: Springer, Cham.
8. Löchte, C., Kunz, H., Schnurr, R., Langhorst, S., Dietrich, F., Raatz, A., ... & Dröder, K. (2014). Form-flexible handling and joining technology (formhand) for the forming and assembly of limp materials. In Procedia CIRP 23.
9. Khalid, M. U., Hager, J. M., Kraus, W., Huber, M. F., & Toussaint, M. (2019, August). Deep Workpiece Region Segmentation for Bin Picking. In IEEE (CASE).
10. Kleeberger, K., Bormann, R., Kraus, W., & Huber, M. F. (2020). A Survey on Learning-based Robotic Grasping. In Journal: Current Robotics Reports.